

An Upper-Bound Approach to Shear Spinning of Cones

Man-soo Kim

원추체의 전단스피닝 가공의 상계하중에 관하여

김 만 수

Summary

The study is concerned with an analysis of the shear spinning process. The upper-bound method is applied to analyze the plastic deformation zone localized in a very small portion of the piece.

Velocity fields and strain rates are derived by considering the adequate deformation mode, and the contact factor is introduced to obtain lower upper-bound power. Then the power and tangential force are determined and calculated for some process variables, and are also compared with the previous literatures.

The comparison shows that the theoretical prediction is in a reasonably good agreement with the experimental results.

NCMENCLATURE

F_t	; Tangential force component in shear spinning, pound	$\bar{\sigma}$; Effective stress, psi
F_r, F_z	; Force components in the radial and axial directions, respectively, pound	$\bar{\sigma}_m$; Mean effective stress, psi
N	; Speed of rotation of the mandrel, rpm	α	; Half the cone angle of the mandrel, deg.
r, θ, z	; Cylindrical co-ordinates	$\theta_0, \bar{\theta}_0$; Ideal geometric angle for deformation zone and its average value, respectively, deg.
x, y, z	; Rectangular co-ordinates	\dot{W}	; Total energy of deformation, pound-inch/min.
D_R	; Roller diameter, $2(r_0 + \rho_0)$	$\dot{\epsilon}$; Strain rate
f	; Feed, inc h/rev. m ; Contact factor	$\dot{\epsilon}_{rz}, \dot{\epsilon}_{zz}, \dot{\epsilon}_{ij}$; Strain rate tensors in cylindrical coordinates
R, R_0, R_i	; Blank radii during operation	U_x, U_y, U_z	; Velocity in X, Y, Z-direction, inch./min.
r_0	; Corner radius of roller, inch	U_r, U_θ, U_z	; Velocity in r, θ , z-direction, inch./min.
ρ_0	; Radius of torus on roller, inch		
ρ, ρ^1	; Radii of curvature of deformation, inch		
t_0, t_f	; Initial and final thickness, respec-		

$\bar{\epsilon}$; Finite effective strain
$\bar{\epsilon}_m$; Mean effective strain in the deformation zone

INTRODUCTION

State of the Art

Spinning is a metal-forming process widely used to fabricate pieces having rotational symmetry.

Because of the simplicity of the operation, spinning offers some distinct economical advantages. Spinning is more economical for producing a small number of pieces than deep drawing because of the low set up time and costs.

Until approximately thirty years ago, the operation of spinning was done manually.

The tool was guided by hand back and forth over the work many times until the material was flatly laid on the mandrel. No instructions were given to the operator concerning the manipulation of the tool. The literature of that time is of little value for this study. The first analytical approach was made by Colding[1](1955). Colding attempts to analyze the stresses and strains during the process of spinning of cones by considering cone spinning as a combination of rolling and extrusion process.

The work of Avitzur[2](1960) was the first to determine the power and tangential force by using upper-bound method. He derived the velocity fields and strain rates and calculated the power and tangential force. His assumed deformation zone in which inlet area is sheared and velocity discontinuity is ignored, is different from actual deformation zone.

In this paper, the inlet flow is considered smooth and so the deformation zone is very similar to actual deformation zone. Slater [11] gives the approximate upper-bound estimates for tangential force during shear spinning of cones

assuming the ideal axi-symmetric deformation. But this assumption is not good enough for the shear spinning process.

Recently Choi [12] (1980) derived the tangential and the other forces by introducing a new deformation model. His analytical results agreed with the experimental data very closely for many working conditions.

General Description

This study deals with the mechanical spinning of cones. However the spinning process can be done by hand when spinning is done by a skilled man who knows by experience how to lay the sheet against the pattern. The advantages of replacing manpower by mechanical power are the same for spinning as for any other industrial process. Mechanical power requires control system, and the controls require a prediction of the forces and motions to which the machine has to be set.

In spinning operations, as they are performed recently, this means the following things:

- (1) The tool can no longer be manipulated back and forth, but must perform the deformation in one pass.
- (2) The rotational speed, the feed, and the head in pressure have to be fixed and preset before spinning is started.

The blank material is a disc or cone and the thickness assumes to be uniform t_0 in case of disc and t_c in case of cone. The disc or cone is mounted on a circular conical mandrel, which is clamped to the head of the spinning machine, and rotated.

A forming roller, the radius $(\rho_0 + \gamma_0)$ is driven on tracks on the bed of the machine parallel to the side of the mandrel, the outer radius R of the cone (Fig. 1) remains the same as the original radius of the disc.

The thickness of the cone is now;

$$t_f = t_0 \sin \alpha$$

$$t_c = t_0 \sin \beta$$

$$t_f = t_c \frac{\sin \alpha}{\sin \beta}$$

In case that blank material is disc, $\beta = 90^\circ$,

$$t_c = t_0$$

$$t_f = t_0 \sin \alpha$$

This type of spinning is called by different names like shear forming, hydro-spinning, etc.

The displacements and strains will be analyzed in more detail.

The material of the roller is hardened tool steel and the roller is mounted on a shaft with ball or roller bearings. There are many shapes of rollers.

The relative position of the roller's axis to the side of the mandrel may differ much in different setups.

From this variety of possibilities, a common roller (Fig.1) which is oriented with its axis parallel to the side of the mandrel was chosen to

be analyzed.

The difference between a successful operation or failure might be sometimes made by the changes in the roller's shape and its positioning.

The strains and stress during a successful operation do not differ much from case to case.

In this analysis, the geometry of the operation have been described mathematically.

The equations of the cone and the roller have also been formulated. And the boundaries of the area of contact between the roller and the cone have then been found.

A solution has been derived for the plastic work of deformation which was based on the deformation theory (Stress-Strain Law) and the solution was computed for the following material

- 1) Homogeneous and isotropic material;
- 2) Incompressible material;

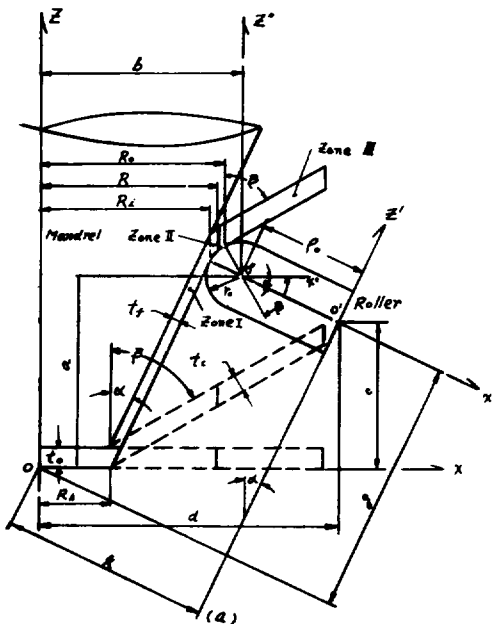


Fig. 1. Deformation in Process

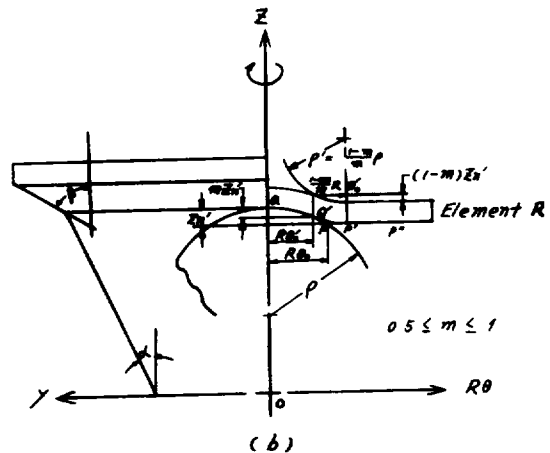


FIG 1 Deformation in Process

Mechanics of Shear Spinning of Cones

$$U_R = U_x \cdot \cos \theta + U_y \cdot \sin \theta$$

$$U_\theta = -U_x \cdot \sin \theta + U_y \cdot \cos \theta$$

Deformation Mode

Deformation mechanism of shear spinning of cones from pre-spun cone blank is shown schematically in Fig. 1 (a), (b).

α is the half cone angle of the mandral and β is the half cone angle of the blank.

The process is characterized by the fact that the R -position of an element in the blank remains the same during deformation and the angular velocity is constant through whole work piece. Moreover, for simplicity, it was assumed that during one revolution of the die and blank the roller holds the same position, and after one complete revolution of the die the roller feeds f sin α to X -direction and f cos α to Z -direction.

This demands that the initial blank thickness to and the final thickness of the cone t_f for die slope angle α is related by the equation.

$$\left. \begin{aligned} t_f &= t_0 \sin \alpha \\ t_c &= t_0 \sin \beta \\ t_f &= t_c \frac{\sin \alpha}{\sin \beta} \end{aligned} \right\} \dots\dots\dots (2-1)$$

The Roller

The geometry of the roller Z_s can be described as [see Fig. 1(a)]

$$[\sqrt{X'^2 + Y'^2} - \rho_0]^2 + Z_s'^2 - r_0^2 = 0 \dots\dots (2-2)$$

$$[\sqrt{(R \cos \theta \cos \alpha - Z_s \sin \alpha - k)^2 + R^2 \sin^2 \theta} - \rho_0]^2 + (R \cos \theta \sin \alpha + Z_s \cos \alpha - g)^2 - r_0^2 = 0$$

$$[\sqrt{(X'' \cos \alpha - Z_s'' \sin \alpha - \rho_0)^2 + Y''^2} - \rho_0^2]^2 + (X'' \sin \alpha + Z_s'' \cos \alpha)^2 - r_0^2 = 0$$

Velocity fields and strain rates

To solve our particular deformation field, the velocity field in the deformation zone was computed first. Because of the deformation mode, the flow line has to be of the form.

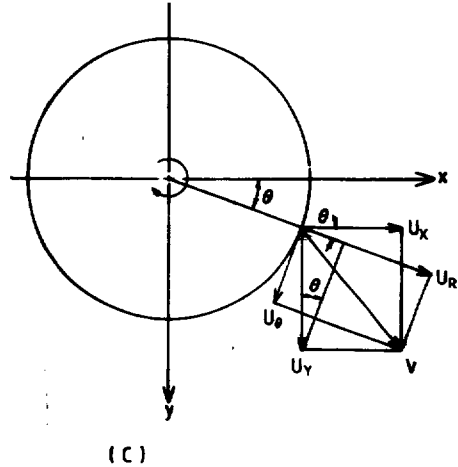


Fig 1 Velocity components in x - y plane

$$\left. \begin{aligned} \Psi(x, y, z) &= x^2 + y^2 = C_1 \\ X(x, y, z) &= Z - Z_D = C_2 \end{aligned} \right\} \dots\dots\dots (2-3)$$

Where Z_D is the Z -value of the curve $QQ'P'P''$ in Fig 1 (b). QQ' is the contacted portion of the roller Z_s with the blank and $Q'P'$ is composed like as Fig.1 (b) to get the same shear strain ϵ_{sz} along the both side of point Q' .

When Q' and P' approaches to P the flow model becomes the similar one proposed by B. Avitzur [2] for shear spinning of cones from flat blank.

In this case velocity discontinuity exists at P and shear loss term which is neglected by B. Avitzur should be involved in the power.

The components of the velocity field, U_x, U_y , and U_z assume the form [10]

$$\left. \begin{aligned} U_x &= \lambda \left(\frac{\partial \Psi}{\partial y} \cdot \frac{\partial X}{\partial z} - \frac{\partial \Psi}{\partial z} \cdot \frac{\partial X}{\partial y} \right) \\ U_y &= \lambda \left(\frac{\partial \Psi}{\partial z} \cdot \frac{\partial X}{\partial x} - \frac{\partial \Psi}{\partial x} \cdot \frac{\partial X}{\partial z} \right) \\ U_z &= \lambda \left(\frac{\partial \Psi}{\partial x} \cdot \frac{\partial X}{\partial y} - \frac{\partial \Psi}{\partial y} \cdot \frac{\partial X}{\partial x} \right) \end{aligned} \right\} (2-4)$$

and from Fig 1(c), one gets

$$\left. \begin{aligned} U_\theta &= U_y \cos \theta - U_x \sin \theta = 2\pi RN \\ U_R &= U_y \sin \theta + U_x \cos \theta \end{aligned} \right\} \dots(2-5)$$

Inserting equations (2-3) into equations (2-4) and (2-5), one gets

$$\left. \begin{aligned} \lambda &= -\pi N \dots\dots\dots(2-6) \\ U_R &= 0 \\ U_\theta &= 2\pi RN \\ U_x &= -2\lambda \left(x \frac{\partial Z_D}{\partial y} - y \frac{\partial Z_D}{\partial x} \right) \dots\dots(2-7) \\ &= -2\lambda \frac{\partial Z_D}{\partial \theta} \\ &= 2\pi N \frac{\partial Z_D}{\partial \theta} \end{aligned} \right\}$$

Noting that $x = \frac{\partial y}{\partial \theta}$ and $-y = -\frac{\partial x}{\partial \theta}$

From the velocity fields of equation (2-7), one gets the strain rates in cylindrical polar coordinates as follows.

$$\left. \begin{aligned} \dot{\epsilon}_{RZ} &= \frac{1}{2} \frac{\partial U_z}{\partial R} = \pi N \frac{\partial^2 Z_D}{\partial R \partial \theta} \\ \dot{\epsilon}_{\theta Z} &= \frac{1}{2R} \frac{\partial U_z}{\partial \theta} = \pi N \frac{1}{R} \frac{\partial^2 Z_D}{\partial \theta^2} \dots\dots(2-8) \\ \text{all other } \dot{\epsilon}_{ij} &= 0 \end{aligned} \right\}$$

The deformation zone is $Q_0 P_0' P_1' Q_1$ in Fig. 2 and $Q_0' Q_1' Q_1' Q_1'$ is the contact line of the roller

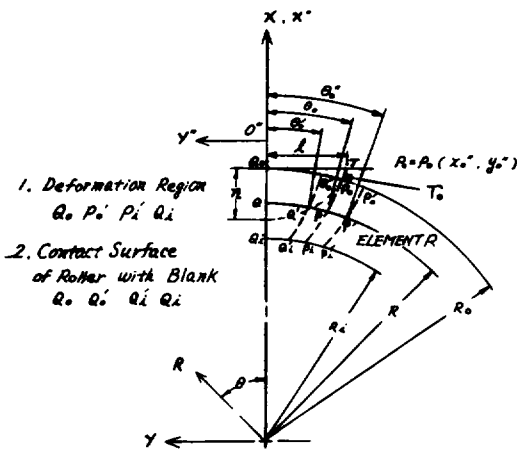


FIG. 2. Approximated Area of Contact.

with the blank.

The Power

The rate of total work done on metal under the deformation zone becomes

$$\dot{W} = \int_{\text{vol}} \frac{\bar{\sigma}}{\sqrt{3}} \sqrt{\left(\frac{\partial U_x}{\partial R}\right)^2 + \left(\frac{1}{R} \frac{\partial U_z}{\partial \theta}\right)^2} dV \dots\dots\dots(2-9)$$

Inserting equations (2-8) into equation (2-9), one gets

$$\dot{W} = \frac{2\pi N t_0 \bar{\sigma}_m}{\sqrt{3}} \left(\int_{\text{area}} \frac{\partial^2 Z_D}{\partial R \partial \theta} \sqrt{1 + \delta^2} dS \right) \dots\dots\dots(2-10)$$

Where

$$\delta = \frac{\partial^2 Z_D}{R \partial \theta^2} / \frac{\partial^2 Z_D}{\partial R \partial \theta} \dots\dots\dots(2-11)$$

and $\bar{\sigma}_m$ is the mean effective stress defined by

$$\bar{\sigma}_m = \int \bar{\sigma} d\bar{\epsilon} / \int d\bar{\epsilon} \dots\dots\dots(2-12)$$

In the case of proportional straining in deformation zone, one gets the average value of δ from equation (2-11)

$$\delta_{\text{avg}} = \int \frac{\partial^2 Z_D}{R \partial \theta^2} dS / \int \frac{\partial^2 Z_D}{\partial R \partial \theta} dS \dots\dots\dots(2-13)$$

Inserting equation (2-13) into equation (2-10), one gets

$$\dot{W} = \frac{2\pi N t_0 \bar{\sigma}_m}{\sqrt{3}} \sqrt{1 + \delta_{\text{avg}}^2} \int \frac{\partial^2 Z_D}{\partial R \partial \theta} dS \dots\dots\dots(2-14)$$

To get the power, the individual integration in equation (2-13) should be calculated.

$$\left. \begin{aligned} I_1 &= \int_{\text{surf.}} \frac{\partial^2 Z_D}{\partial R \partial \theta} dS \\ &= \int_{\theta} \int_R \frac{\partial^2 Z_D}{\partial R \partial \theta} R dR d\theta \end{aligned} \right\} \dots\dots(2-15)$$

Since $\frac{\partial^2 Z_D}{\partial R \partial \theta}$ changes appreciably for slight change of R, R itself can be considered as constant

$$(R \doteq \bar{R} = \frac{R_1 + R_0}{2} \text{ Therefore}$$

$$\begin{aligned}
 I_1 &= R \int_0^{\theta_0} \int_R \frac{\partial^2 Z_D}{\partial R \partial \theta} dR d\theta \\
 &= R \int_{\theta=0}^{\theta_0} \frac{\partial Z_D}{\partial \theta} \Big|_{R=\text{lower limit}}^{R=\text{upper limit}} d\theta \\
 &= R [Z'_n |_{R=R_0} - Z'_n |_{R=R_i}] \\
 &= R f \cos \alpha (1 - \tan \alpha \cot \beta) \dots (2-16)
 \end{aligned}$$

Noting that

$$Z'_n |_{R=R_i} = 0 \dots (2-17)$$

and

$$\begin{aligned}
 Z'_n |_{R=R_0} &= f \cos \alpha (1 - \tan \alpha \cot \beta) \\
 I_2 &= \int_{\text{surf.}} \frac{\partial^2 Z_D}{R \partial \theta^2} dS \\
 &= \int_R \int_{\theta} \frac{\partial^2 Z_D}{R \partial \theta^2} R d\theta dR \\
 &= \int_R \left(\frac{\partial Z_D}{\partial \theta} \Big|_{\theta=0}^{\theta=\theta_0'} + \frac{\partial Z_D}{\partial \theta} \Big|_{\theta=\theta_0''}^{\theta=\theta_0'} \right) dR \\
 &= \int_R 2 \frac{\partial Z_s}{\partial \theta} \Big|_{\theta=0}^{\theta=\theta_0'} dR \dots (2-18)
 \end{aligned}$$

Noting that, from the flow model and Fig. 1 (b),

$$\frac{\partial Z_D}{\partial \theta} \Big|_{\theta=0}^{\theta=\theta_0'} = \frac{\partial Z_D}{\partial \theta} \Big|_{\theta=\theta_0''}^{\theta=0''}$$

and

$$\frac{\partial Z_D}{\partial \theta} \Big|_{\theta=0}^{\theta=\theta_0'} = \frac{\partial Z_s}{\partial \theta} \Big|_{\theta=0}^{\theta=\theta_0'}$$

Also from Fig. 1 (b), one gets

$$\frac{\partial Z_s}{R \partial \theta} \Big|_{\theta=0} = 0 \dots (2-19)$$

and

$$\begin{aligned}
 \frac{\partial Z_s}{R \partial \theta} \Big|_{\theta=\theta_0'} &\doteq \frac{2mZ'_n}{R\theta_0'} \\
 &\doteq \frac{2\sqrt{m}Z'_n}{R\theta_0} \dots (2-20)
 \end{aligned}$$

Noting that, from Fig. 1 (b),

$$\rho \doteq \frac{(R\theta_0')^2}{2mZ'_n} \doteq \frac{(R\theta_0)^2}{2Z'_n} \dots (2-21)$$

Where $0.5 \leq m \leq 1$.

Inserting equations (2-19) and (2-20) into

equation (2-18), one gets

$$I_2 = \int_R \frac{4\sqrt{m}Z'_n}{\theta_0} dR \dots (2-22)$$

Inserting the average value of Z'_n and θ , one gets

$$I_2 = \frac{4\sqrt{m}(Z'_n)_{\text{avg}}}{\bar{\theta}_0} \gamma_0 (\cos \alpha - \cos \beta) \dots (2-23)$$

Where $\bar{\theta}_0$ is the average angle of the deformation zone shown by θ_0 in Fig. 2

Noting that

$$\begin{aligned}
 (Z'_n)_{\text{avg}} &= [Z'_n |_{R=R_i} + Z'_n |_{R=R_0}] / 2 \\
 &= \frac{1}{2} f \cos \alpha (1 - \tan \alpha \cot \beta) \dots (2-24)
 \end{aligned}$$

Inserting the equations (2-16) and (2-23) into the equation (2-13), one gets

$$\begin{aligned}
 \partial \text{avg} &= \frac{I_2}{I_1} \\
 &= \frac{2\sqrt{m} \gamma_0 (\cos \alpha - \cos \beta)}{R \bar{\theta}_0} \dots (2-25)
 \end{aligned}$$

Inserting equations (2-16) and (2-25) into the equation (2-14), one gets the required total power

$$\begin{aligned}
 \dot{W} &= \frac{2\pi N t_0 \bar{\sigma}_m}{\sqrt{3}} R f \cos \alpha (1 - \tan \alpha \cot \beta) \\
 &\quad \sqrt{1 + \delta^2 \text{avg}} \dots (2-26)
 \end{aligned}$$

Where δavg is given by equation (2-25).

One can get the angle for deformation $\bar{\theta}_0$ from equation (2-2) by inserting R_0 to R and h to Z_s .

$$\begin{aligned}
 &[\sqrt{(R_0 \cos \bar{\theta}_0 \cos \alpha - h \sin \alpha - k)^2 + R_0^2 \sin^2 \bar{\theta}_0} \\
 &\quad - \rho_0]^2 + (R_0 \cos \bar{\theta}_0 \sin \alpha + h \cos \alpha - g^2) \\
 &\quad - r_0^2 = 0 \dots (2-27)
 \end{aligned}$$

Where, from the geometry of Fig. 1 (a).

$$\begin{aligned}
 h &= a + r_0 \sin \beta - f \cos \alpha (1 - \tan \alpha \cot \beta) \\
 k &= d \cos \alpha - c \sin \alpha \\
 g &= c \cos \alpha + d \sin \alpha \\
 c &= a - \rho_0 \sin \alpha \\
 d &= b + \rho_0 \cos \alpha \\
 b &= R_0 + \rho_0 \cos \beta
 \end{aligned}$$

$$a = (b - \frac{r_0}{\cos \alpha} - R_k) / \tan \alpha$$

Inserting the above equations into equation (2-27), one gets

$$\begin{aligned} & \left\{ \sqrt{R_0 \cos \alpha \cos \bar{\theta}_0 - (h-a) \sin \alpha - b \cos \alpha} \right. \\ & \quad \left. - \rho_0 \right\}^2 + R_0^2 \sin^2 \bar{\theta}_0 - \rho_0^2 \\ & + [R_0 \sin \alpha \cos \bar{\theta}_0 + (h-a) \cos \alpha \\ & \quad - h \sin \alpha]^2 - r_0^2 = 0 \dots \dots \dots (2-27') \end{aligned}$$

The average value of the angle for the deformation zone $\bar{\theta}_0$ is approximately given by

$$\bar{\theta}_0 = \cos^{-1} \left\{ \frac{l^2}{n^2} - \sqrt{1 + \left(\frac{l}{R_0}\right)^2 \left(\frac{l^2}{n^2} - 1\right)} \right\} \dots \dots \dots (2-28)$$

Where

$$\begin{aligned} l^2 &= r_0^2 \sin^2 \beta - r_1^2 + 2\rho_0 \\ & \quad [\sqrt{r_0^2 - (-r_0 \cos \beta \sin \alpha + r_1 \cos \alpha)^2} \\ & \quad - (r_0 \cos \beta \cos \alpha + r_1 \sin \alpha)] \\ n &= \sqrt{r_0^2 - r_1^2} - r_0 \cos \beta \\ r_1 &= r_0 \sin \beta - f \cos \alpha (1 - \tan \alpha \cot \beta) \end{aligned}$$

The derivation of equation (2-28) is shown in the Appendix.

In the case of cone spinning from flat blank; $\beta = \frac{\pi}{2}$, one gets

$$\dot{W} \Big|_{\beta = \frac{\pi}{2}} = \frac{2\pi N t_0 \bar{\sigma}_m}{\sqrt{3}} R f \cos \alpha \sqrt{1 + \delta \text{avg}^2} \dots \dots \dots (2-26')$$

Where

$$\delta \text{avg} = \frac{2\sqrt{m} r_0 \cos \alpha}{R \bar{\theta}_0} \dots \dots \dots (2-25')$$

and

$$\bar{\theta}_0 = \cos^{-1} \left\{ \frac{l^2}{n^2} - \sqrt{1 + \left(\frac{l}{R_0}\right)^2 \left(\frac{l^2}{n^2} - 1\right)} \right\} \dots \dots \dots (2-28')$$

$$\begin{aligned} l^2 &= r_0^2 - (r_0 - f \cos \alpha)^2 + 2\rho_0 \\ & \quad [\sqrt{r_0^2 - (r_0 - f \cos \alpha)^2 \cos^2 \alpha} \\ & \quad - (r_0 - f \cos \alpha) \sin \alpha] \\ n &= \sqrt{r_0^2 - (r_0 - f \cos \alpha)^2} \end{aligned}$$

The Tangential Force

It will be shown that the greatest portion of the power is absorbed through the tangential component of the force acting between the roller and cone.

The force might be resolved to its three following components: Tangential Force (F_t), Radial Force (F_r), and Axial Force (F_x). In general, the power is the sum of the forces multiplied by the velocities directed parallel to this forces.

This can be written as

$$\dot{W} = F_t \cdot U_\theta + F_r \cdot U_r + F_x \cdot U_x$$

where U_θ is the circumferential velocity

U_r is the radial velocity

U_x is the axial velocity

The roller does not move in the radial direction, so $U_r = 0$.

It follows that

$$\begin{aligned} \dot{W} &= F_t \cdot U_\theta + F_x \cdot U_x \\ &= \dot{W}_t + \dot{W}_x \end{aligned}$$

where \dot{W}_t is the tangential power

\dot{W}_x is the axial power

By Avitzur's degree thesis, the power consumed by the feed force is less than 7% of the total power in a typical case.

So we can neglect the feed power and the power consumed can be regarded as done entirely by the tangential force.

One now gets

$$\dot{W} = F_t \cdot U_\theta$$

where $U_\theta = 2\pi \bar{R} N$

And the tangential force component on the roller may be written in the form of

$$F_t = \frac{\dot{W}}{2\pi \bar{R} N} = \frac{t_0 \bar{\sigma}_m}{\sqrt{3}} \cdot f \cdot \cos \alpha \cdot \sqrt{1 + \delta \text{avg}^2}$$

RESULTS AND DISCUSSION

In Fig. 3-9. These theoretical results are com-

pered with the other thesis' results. (J.C. Choi and Avitzur, B. 1980, 1960)

The effects of each of the parameters, Feed f , cone included angle $2\alpha_0$, cone radius R_0 , roller round off radius r_0 , and roller radius ρ_0 on the tangential force, are given in the figures.

When one knows these five parameters for actual case, one finds the value of the weighted tangential value from the suitable figures.

For the analytical study, a displacement fixed was postulated, which gave the strain-rates field. The strain-rates field satisfies automatically the compatibility conditions.

In geometrical respect, Avitzur neglected the shear loss term along in Fig 1-b, which violates the upper-bound theorem.

The shear loss along is pretty high and can not be neglected on the calculation of the power in usual upper-bound solution based on the kinematically Admissible Velocity Fields.

In this study, as shown in Fig 1-b, it was assumed that there is no shear but more deformation zone. The tangential force increases almost linearly as the feed increases when other parameters are constants.

The effect of contact factor m , are shown in figures. They show that for larger contact factor, larger tangential force is required but the difference is very small. And also the figures show that larger cone radius requires smaller force.

Fig 6, 7, show the comparison between the Choi's theoretical results and the present results. When $m = 0.5$, two results coincide very closely but when $m = 1.0$, the present results are larger than Choi's results and the Choi's results are closer to the experimental data.

However in the range of small feed, the in-

fluence of contact factor is negligible.

Fig 8. shows comparison between Avitzur's theoretical results and the present results.

When $m = 0.5$, Avitzur's results are usually larger than the present results. It is natural that Avitzur's results should be larger than the present results according to the reason that Avitzur neglected the shear term.

It is interesting to note that there are reasonable agreements between the present theory and the experimental data obtained from previous literatures.

There is an excellent agreement between this deformation theory and the experimental results as shown in Figures.

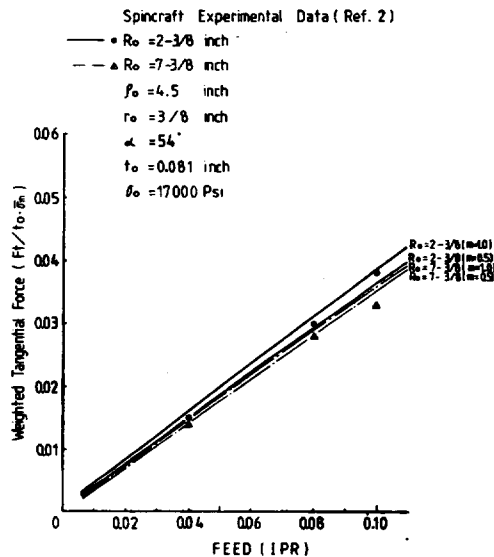


Fig 3 Weighted Tangential Forces versus Feed ($\alpha = 54^\circ$)

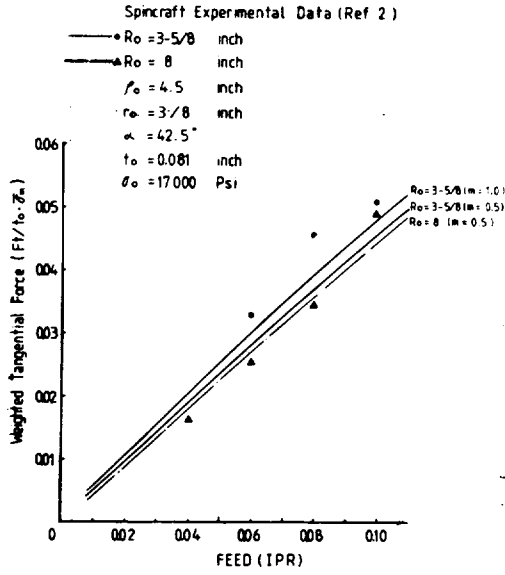


Fig 4 Weighted Tangential Forces versus Feed ($\alpha = 42.5^\circ$)

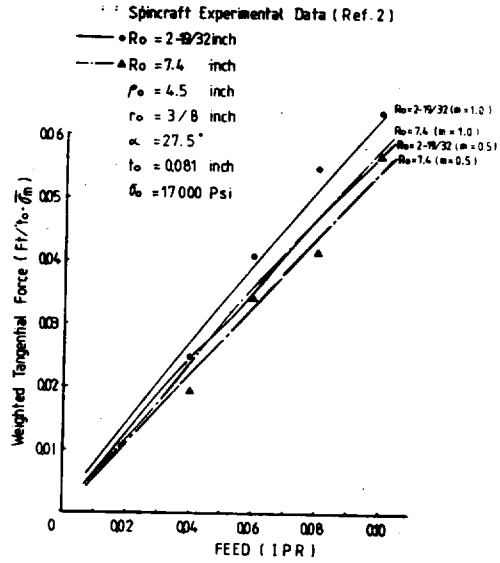


Fig 5 Weighted Tangential Forces versus Feed ($\alpha = 27.5^\circ$)

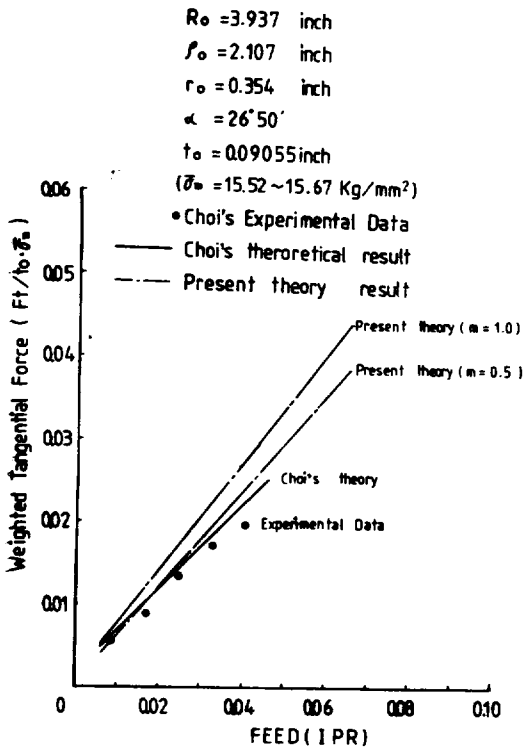


Fig 6 Weighted Tangential Forces versus Feed ($\alpha = 26^\circ 50'$, $t_o = 0.126$ in)

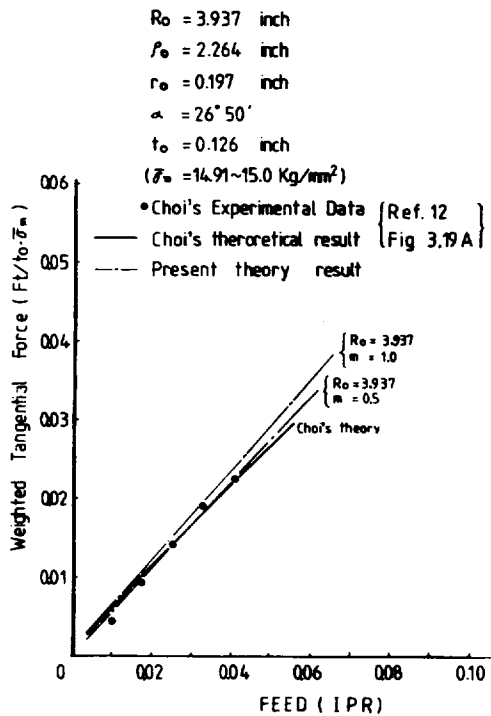


Fig 7 Weighted Tangential Forces versus Feed ($\alpha = 26^\circ 50'$, $t_o = 0.09$ in)

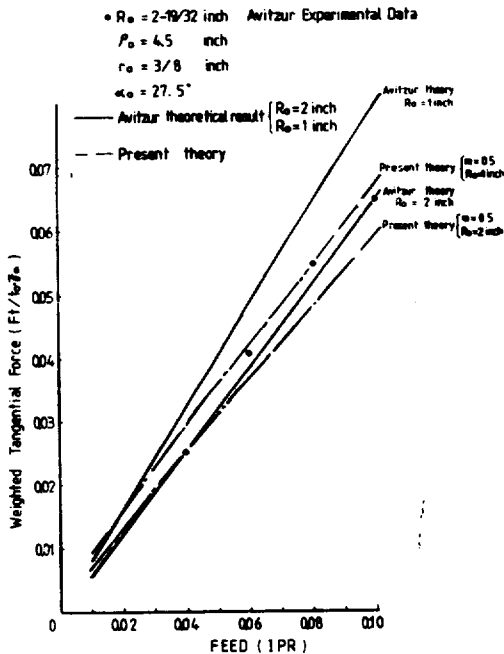


Fig 8 Weighted Tangential Forces versus Feed

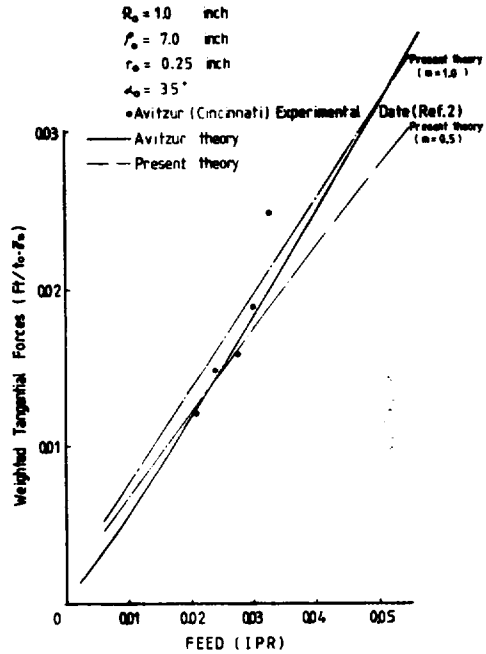


Fig 9 Weighted Tangential Forces versus Feed

Literatures Cited

1. Avitzur, B.C.T. Yang, (1960). "Analysis of Power Spinning of Cones," Journal of Engineering for Industry, TRANS. ASME, Series B, Vol. 82, pp.231-245.
2. Colding, B.N.(1911) "Shear Spinning," ASME Paper No.59-Prod.-2.
3. Choi (J.C.)(1980) "A Study on the Mechanics of Shear Spinning of Cones" Ph.D. Thesis, Pusan National University.
4. Hayama, M.T. Murota, H.Hudo, (1963, 1965, 1966) "Study of Shear Spinning,"

1st Report, 1963	}—Trans. JSME
2nd Report, 1965	
3rd Report, 1966	
5. Kalpakcioglu, S (1961) "On the Mechanics of Shear Spinning," Journal of Engineering for Industry, TRANS. ASME, Series B, pp.125-130.
6. S. Kalpakcioglu, "A Study of Shear-Spinnability of Metals," Journal of Engineering for Ondustry, TRANS. ASME, Series B, pp.478-484.
7. Richard L. Kegg, (1951) "A New Test Method for Determination of Spinnability of Metals," Journal of Engineering for Ondustry, TRANS. ASME, Series B, pp.119-124, (paper No.60-Prod.-3).
8. Kobayashi, S.I. K. Hall, E. G. Thomsen, (1961). " A Theory of Shear Spinning of Cones," Journal of Engineering for Ondustry, TRANS. ASME, Series B, pp.485-495.
9. Kobayashi, S (1963) "Instability in Conventioal Spinning of Cones," Journal of Engineering for Industry, TRANS. ASME. Series B, Vol. 85, pp.44-48.
10. Rouse H. (1959) et., "Advanced Mechanics of Fluids," Section 21 Chap.2 John Wiley & Sons, Inc., N.Y.
11. Slatter R.A.C. (1978) "Spin-Forging of Sheet

Metal Cones Having Various Cone Angles from 70-30 Brass and Commercially Pure Aluminum", Proceedings of IUTAN Symposium, Springer Verlag,

12. Sortais, H.C.S. Kobayashi, E.G. Thomsen, "Mechanics of Conventional Spinning", Journal of Engineering for Industry, TRANS. ASME, Sries B, Vol. 85, pp.346-350.

<국문초록>

원추체의 전단스피닝 가공의 상계하중에 관하여

金 萬 守

이 연구는 전단스피닝에 대한 이론 해석을 하고 종전 결과의 원추의 스피닝 소요 동력보다 더 정확한 동력을 구해보려고 시도했다. 가공물의 미소부분의 소성 변형 영역을 해석하기 위하여 상계법을 적용하였다. 이 변형역의 변형모형을 아비츄의 변형모델과 달리 새 모델을 가정하여 속도장파 변형 속도를 유도하였다.

그리고 최소 상계력을 구하기 위하여 접촉 계수를 도입하였다. 그 부하와 접선력을 과정 변수를 써서 구하고 종전 결과와 비교하여 필자의 모델에 의한 결과가 실험결과와 잘 일치되었다.